Main/Tail Rotor Interaction under Ground Effect Using DLR 3D Free Wake Code

Jianping Yin, Jan Delfs

DLR, Institute of Aerodynamics and Flow Technology,
Technical Acoustics Division,
Lilienthalplatz 7, 38108 Braunschweig, Germany

Abstract

The prediction of the ground effect on rotor aerodynamics remains a challenging task for all wake models because of the complicated influence of the ground on the wake development. A numerical simulation of main rotor and tail rotor interaction operating in ground effect was carried out with two different ground models, an image and a surface singularity model. An unsteady free wake 3-D panel code developed at DLR has been extended to account for the ground effect. The effect of the ground on rotor interference versus height above ground was examined on the basis of the main and tail rotor wake development and corresponding loads. The study was conducted for a simultaneously rotated main/tail rotor configuration in hover and forward flight. The results with two different ground models were compared. The problem of using a surface singularity model is discussed.

1. Introduction

The knowledge of the aerodynamic environment at helicopter rotors is of basic interest when analysing the interaction aerodynamics and the aeroacoustics of helicopters.

The accurate prediction of helicopter main rotor (MR) and tail rotor (TR) interaction still remains an important issue in rotorcraft design, because the interactional phenomena affect rotorcraft performance, handling qualities, vibration and noise. Various studies on main/tail rotor interaction were carried out [e.g.1~4]. Quackenbush et al [1] studied the MR/TR interaction with special emphasis on the generated acoustics. The theoretical approach was to evaluate the flow field in the inlet plane of the TR disc without simulating the TR or its wake and then using this data to compute the flow field for the TR with high resolution. They note the importance of simulating the full-span wake of the MR to correctly capture the TR acoustics. Interaction of MR/TR is also the subject of the work of Baron & Boffadossi [2] where the aerodynamics are investigated using a lifting surface representation for the blade and a Lagrangian vortex lattice free wake. Aerodynamic interaction between multiple rotor configurations was investigated by Bagai & Leishman [3] where a full-span wake with a roll-up concept is used to simulate the free tip vortices (as a total representation of the wake). Employing a combination of unsteady panel method and acoustic analogy method, Yin & Ahmed [4] studied aerodynamic interaction and the noise generated by a generic two-blade MR/TR configuration in hover and a four-blade MR with a two-blade TR configuration in climb mode. Their results demonstrated that the TR wake was strongly distorted by the MR interaction. A fully interactive free wake model was used.

It is even more challenging is to simulate the behaviour of MR/TR interaction in ground effect because of the complicated mutual interference of the ground on the development of MR&TR wake. Earlier studies in this area were mainly concentrated on wind tunnel tests [e.g. 5] and only limited investigations of simulated conditions were carried out. In recent work of Griffiths & Leishman [6], a detailed study of dual-rotor interference and ground effect was made by using a free-vortex wake model. In this study, the free-vortex wake model based on a relaxation scheme was used. Their wake analysis requires an initial condition and wake periodicity is enforced as a boundary condition, assuming that the wake structure repeats itself each and every rotor revolution. The ground was simulated using both method of images and surface singularity method.

The paper is structured as follows. At first, the aerodynamic model of DLR's 3D unsteady free wake panel code is introduced. The extension of the code to account for the ground effect is then applied for a simultaneously rotated MR/TR configuration in hover and forward flight under ground effect. The results with two different ground models were compared. The problem of using a surface singularity model is discussed.

2. Description of the Method

2.1 The Aerodynamic Model

The aerodynamic code **UPM-Mantic** [4] is based on an unsteady 3-D full-span free wake panel method and can be used to treat two simultaneously turning multi-blade rotors each with a (full-span) free wake in any arbitrary motion.

2.1 Model of Lifting Rotor Blade

The model of the lifting rotor blade consists of following elements (**Fig. 1**):

a) A source/sink distribution over the blade surface to simulate the displacement effect of blades with *finite* thickness.
b) A *prescribed* weighting function for the vortex strength over the blade chord to account for the blade lift.
c) A short zero-thickness elongation of the trailing edge along its bisector *(Kutta panel)* to satisfy the Kutta condition. The satisfaction of the flow tangency condition on the Kutta panel fixes the total strength of the circulation in the blade section; its variation over the blade chord is given by b) above. The orientation of the Kutta panel determines the direction of the emission of a wake element at the time of its release from the blade trailing edge.

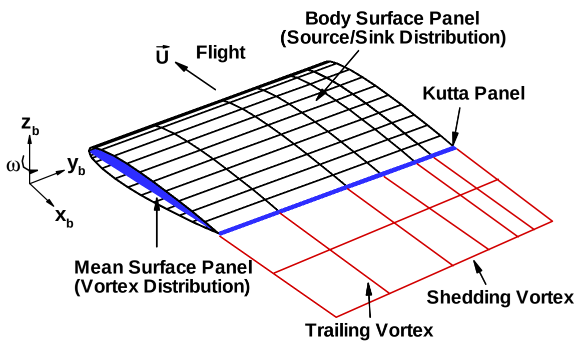

Fig. 1 Numerical Model of a Blade and Wake

2.2 Model of Free Wake Generation

The model of free wake consists of following steps:

a) At the start of the computation there are no MR and TR wakes present.
b) After the first computation step, all rotor blades move to a new position with a velocity which is relative to the ground fixed frame of reference and consists of translation, rotation and other motion. **Fig.1** shows the wake strip comprising a series of quadrilateral ring vortices after having been released from the downstream edge of the Kutta panel. The spanwise variation of the circulation on this new row of wake panels is the same as that on the Kutta panels and will keep unchanged throughout the whole computations.
c) After each computation step, a new wake strip is created and added to the previous wake. The whole wake surfaces are then freely deformed according to the locally induced velocity.
d) With the generation of the wake its induction effect is included to satisfy the flow tangency condition for the next computation step.

A full-span free wake is generated in this manner step by step behind the blades as the computation proceeds.

The free wake analysis requires no initial condition and is a fully interactive free wake model.

2.3 Numerical Implementation

Problem formulation is based on a reference fixed with the ground (**Fig. 2**). All the blade motions and blade positions are referred to this frame of reference. The relationship between the ground fixed and a blade-fixed frame of reference can be expressed with the help of the transformation matrices. The details of these matrices are given in [4].

The blade and mean surface of MR and TR are first partitioned into small planar surface elements (panels), which carry a source/sink or doublet distribution of unknown strength, σ_j, μ_j respectively. After the boundary condition of flow tangency imposed on the MR- or TR surface is satisfied with full consideration of the mutual interaction between the MR/TR blades and their free wakes, a system of *linear* algebraic equations can be written as:

$$\sum_{j=1}^{m_s} A_{ij}\sigma_j + \sum_{j=1}^{n+m_k} B_{ij}\mu_j = R_i - \sum_{j=1}^{p} C_{ij} Z_j$$

$$i = 1,2,3 ...... \qquad m_s + m_k \tag{1}$$

Whose solution gives the strength of singularities (source/sink or doublet) on all collocation points ($m_s + m_k$) of MR and TR after each computation (time) step. Hereby m_s is the total number of panels on the MR- and TR, n the total number of panels on the MR/TR-blade mean surface, and m_k the total number of MR- and TR Kutta panels. The number of panels on the blade surface and the number of Kutta panels remains constant. The number of wake panels p, however, increases as the computation progresses. The above system of equations is solved iteratively for each time step. A_{ij}, B_{ij} and C_{ij} are the mutual „influence coefficients" of the (surface and wake) panels. Since the relative position of the MR/TR blades and their wakes changes after each time step, these influence coefficients need to be updated after each computation step.

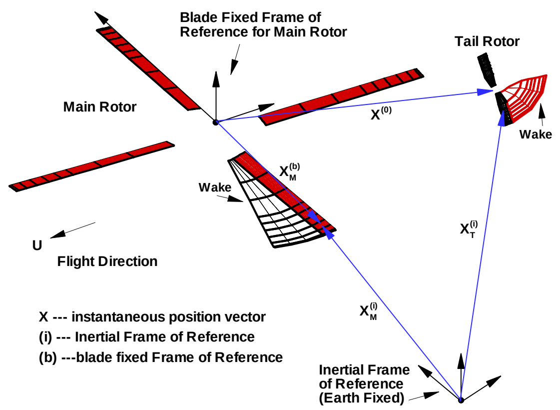

Fig. 2 Blade Fixed- and Inertial Frame of Reference

The pressure on the blade surface is calculated using the unsteady Bernoulli equation. The non-linearity of the problem stems from the a priori unknown spatial location of the wakes. An additional complexity in the case of MR/TR operation arises due to the relative motion between the MR and TR blades, whose consideration is essential to correctly capture the interaction effects.

The methods to reduce computation time which was introduced in [7] are again used.

3. Ground plane models

Simulation of the ground flow is another important feature to be incorporated in the code. With the limitation that flow over the body and ground is assumed to be inviscid, two different ground models, 'Mirror image model or Method of images model (MIM)' and 'Source panel model (SPM)' are implemented in current DLR's UPM-Mantic code.

The MIM approach creates a 'mirror image' of the above-ground rotor and its wake, and induced velocity contributed from the image rotor and wake will be incorporated in satisfying the boundary condition on the blade and in updating the free wake geometry. The boundary condition on the ground plane is implicitly satisfied due to using the image system. The image systems are quite efficient for analyzing problems of simple geometry.

The SPM method is to represent the ground as a system of source panels distributed on the ground plane, like the system used on the blade surface. The boundary condition on the ground plane has to be explicitly satisfied. The source distribution on the ground plane is determined to satisfy the normal velocity boundary condition. The SPM offers more generality and flexibility in terms of configurations that can be modelled, but the occurrence of free wake filaments passing directly through the panelled plane can only be avoided when in theory extremely high level resolution of the wake and panels would be used. In practice this level of refinement would hardly be worth the increase in CPU time [8]. A simple treatment is implemented, in which the coordinates of wake elements are replaced by that of the closest ground panel coordinates once the wake elements moving across the ground panel are identified.

4. Numerical Simulation and Discussion

A single hovering rotor in ground effect (IGE) is studied first. The ground is modelled using the MIM and SPM methods. A quantitative comparison is made with both the shadowgraph flow-visualization results of Light [9] and simulation results of Griffiths & Leishman [6].

The MR/TR is then simulated using the MIM method. The numerical simulation results with a generic two-blade MR and two-blade TR configuration as well as BO105 MR/TR are presented.

4.1 Single hovering rotor IGE

2-blade Caradonna –Tung rotor

The Caradonna and Tung [10] rotor is chosen at first. The rotor consists of two rectangular and untwisted blades with a NACA 0012 profile. Each blade is discretised in this case by 26 panels along the profile contour and 8 panels along the span, totally 204 panels for one blade. The results are obtained for an azimuth step size of 11.25 degrees and the rotor is impulsively started. Both MIM and SPM model is used to simulate the ground effect. The different ground positions are computed.

Fig.3 demonstrates the side views of the free wakes of the rotor operating at different ground positions. The position of the ground is given in the figure. In each case, the rotor collective pitch is held constant at its hover out of ground effect (OGE) value. The free wake snap shot for the rotor OGE is also given for comparison. Only the wake tip filaments are plotted. The results are given after 12 free wake turns.

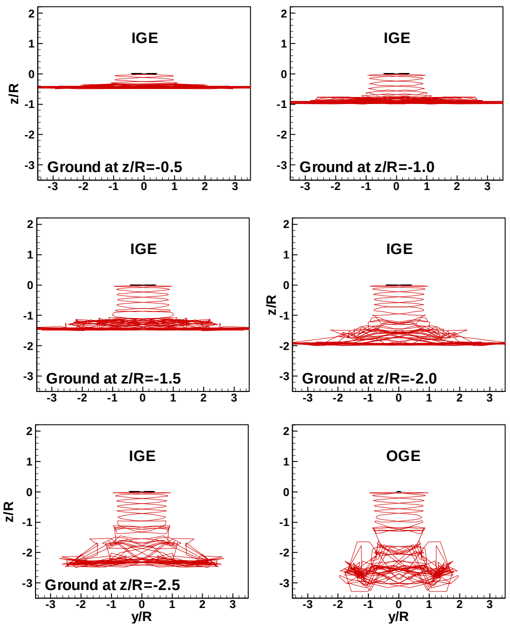

Fig. 3 Side view of the free wake for Caradonna rotor hovering IGE (MIM) and OGE, showing the ground effect at different ground plane positions.

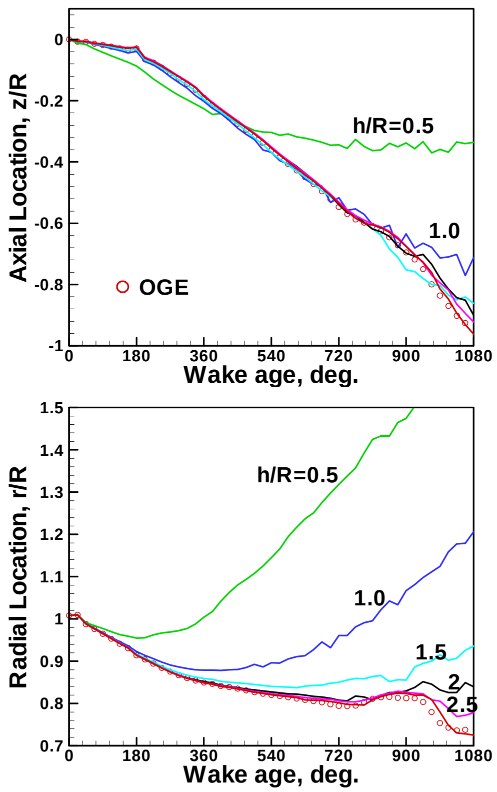

Fig. 4 Comparison of the wake axial and radial locations with respect to different h/R for 2-blade Caradonna-Tung rotor

Due to the ground induced blockage of the airflow under the rotor, the changing of wake system in ground effect (IGE) case is already observed starting from h/R=2.5 and becomes more pronounced with decreasing the rotor height, h, from the ground. The wake sprays over ground and extends radially away from the rotor with increasing the rotor turns.

Fig.4 shows a comparison of the wake axial and radial locations with respect to different h/R. Also plotted in the figure are the results OGE, which are represented by circles. For the large rotor/ground distance, the tip vortex descent rate is constant up to second blade passage at about 180deg. The descent rate increases and then remains constant to 720 deg. beyond which the tip vortex location shows more variation with increasing azimuth. But the axial descent of the tip vortices is significantly decreased when they are close to the ground. The ground effect on the tip vortex location is most evident in radial direction. For the small rotor/ground distance, the radial geometry of the tip vortex contracts for a short period and then expands rapidly.

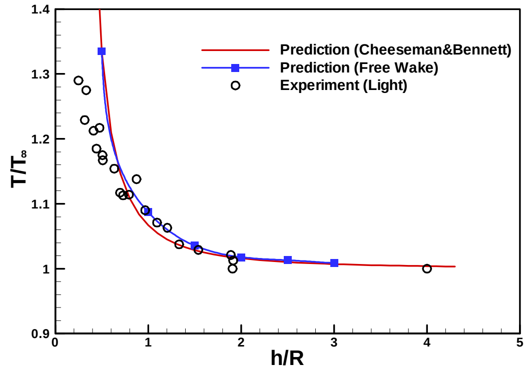

Fig. 5 Comparison of measured and predicted thrust in ground effect

Fig. 5 shows the ratio of the rotor thrust IGE to the thrust OGE plotted as a function of the distance from the ground plane for a constant collective pitch. In addition, the measured data obtained from Light test with a Lynx tail rotor and the data based on the method of Cheeseman and Bennett [11] is also plotted in Fig. 5. The prediction based on the free wake has a better correlation with test data for h/R>0.6 than Cheeseman & Bennett method's since in their method the characteristics of the rotor blade and the operation condition is not taken into account.

4-blade Lynx tail rotor

The 4-blade Lynx tail rotor has constant chord, untwisted blades with a radius of R=1.105 m and NPL9615 airfoil. More information on this rotor is given in [9].

In all simulations, 208 panels per blade are employed including 26 panels around the blade profile and 8 panels along the span. The results are obtained for an azimuth step size of 11.25 degrees and the rotor is impulsively started. The method of images is used to simulate the ground effect and the ground plane is located at z/R=-0.84.

To show the wake and ground interaction on the development of the rotor wakes, the side view of a snap-shot of the free wakes is illustrated in Fig.6. The free wake snap shot for the rotor OGE is also given for comparison. The results are given after 12 free wake turns.

The wake spraying over ground and extends radially away from rotor is clearly simulated.

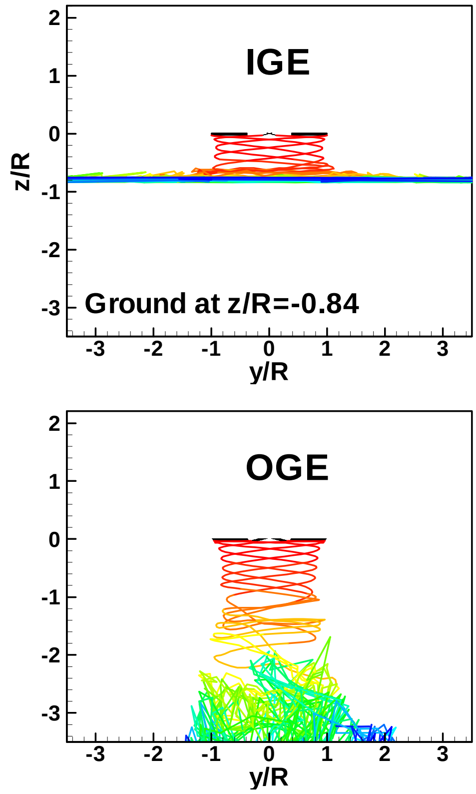

Fig. 6 Side view of the free wake for Lynx tail rotor hovering IGE (MIM) and OGE, showing the ground effect at z/R=-0.84.

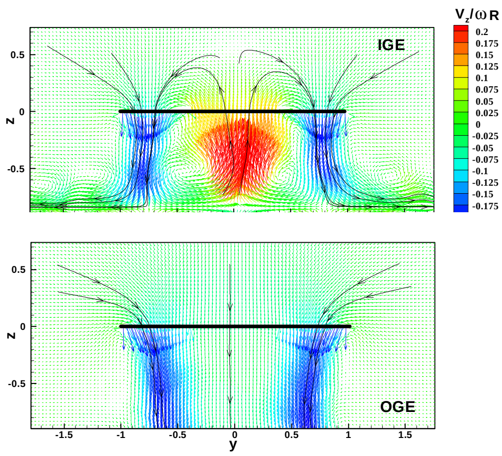

Fig. 7 The induced velocity vector contour and stream line plots

A 2-D vector plot of induced velocity, velocity contour and stream lines (Vz component as contour value) are depicted in Fig.7 in the area around the rotor. The IGE case demonstrates that the interference of the ground surface with the airflow pattern of the rotor system reduces the downward velocity of the flow, especially outboard of the rotor disc. It also shows the tip vortex contracts for a short period, and then expands rapidly. The reduction of induced velocity will result in less induced drag and a more vertical thrust.

In the inner part of rotor disc, especially near the root, flow recirculation is observed. The reason for the up wash in the inboard part of the rotor disc may be introduced due to initial vortex and artificial cutout of the blade root. The sign of the inner vortex sheet is opposite to the tip vortex. Therefore, the vortices located near the root tend to move upward. The location of the root vortex is balanced by downward induced velocity from the tip vortex, but due to the reduced velocity induced by the tip vortex IGE, the final location is closer to the rotor disc than OGE. The weak instability caused by inner vortex sheet is observed in the time history of the rotor thrust.

The variation of thrust over the azimuth can also be used to analyze the wake/ground interaction process. **Fig.8** gives comparison of rotor thrust time history both IGE and OGE. Both cases run at same collective pitch. With the start of the rotor revolution, the thrust increases steeply and then settles down to a fairly constant value later for both IGE and OGE. This thrust build up is due to the strong starting vortex which is shed off the blade trailing edge at the impulsive start of the rotor. With the progress of the computation, the vortices move away from the blades and the normal wake structures are established. The thrust curves converge toward a constant value. As was mentioned, the small wiggle in time history IGE is observed.

It shows rotor thrust increases due to the fact that induced velocity decreases close to the ground.

Fig.9 shows a quantitative comparison of the predicted wake geometry to the shadowgraph flow visualization results of Light as well as Griffiths & Leishman's free vortex prediction (courtesy of Griffiths & Leishman). The good prediction in axial location is obtained for both the predictions. The characteristics in the radial location are captured.

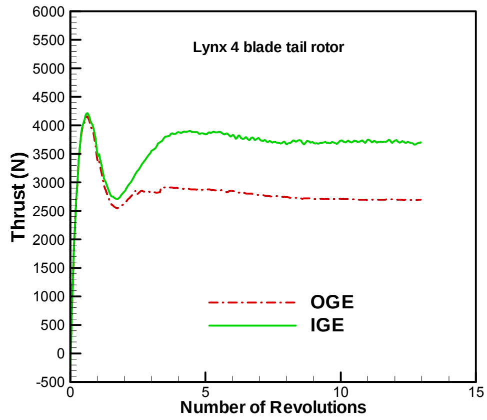

Fig. 8 Comparison of rotor thrust time history both IGE and OGE

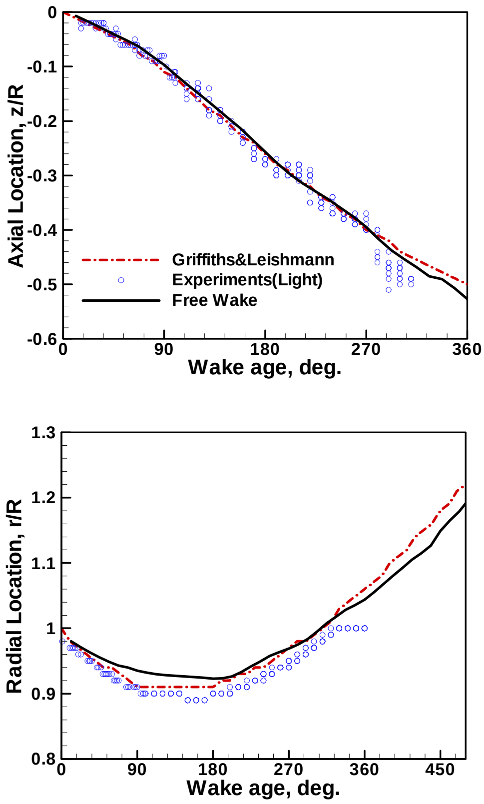

Fig. 9 Comparison of measured and predicted tip vortex axial and radial location IGE

The SPM method is also used to model the rotor and ground interaction in which the ground is represented as a system of source panels. The ground size is chosen as a rectangle with the size 6.5R on each side. The center of the rectangular plane coincides with the center of the rotor. The ground plane is located at z/R=-0. 84. Two different panel grid sizes, Δ=0.16R and Δ=0.32R are used.

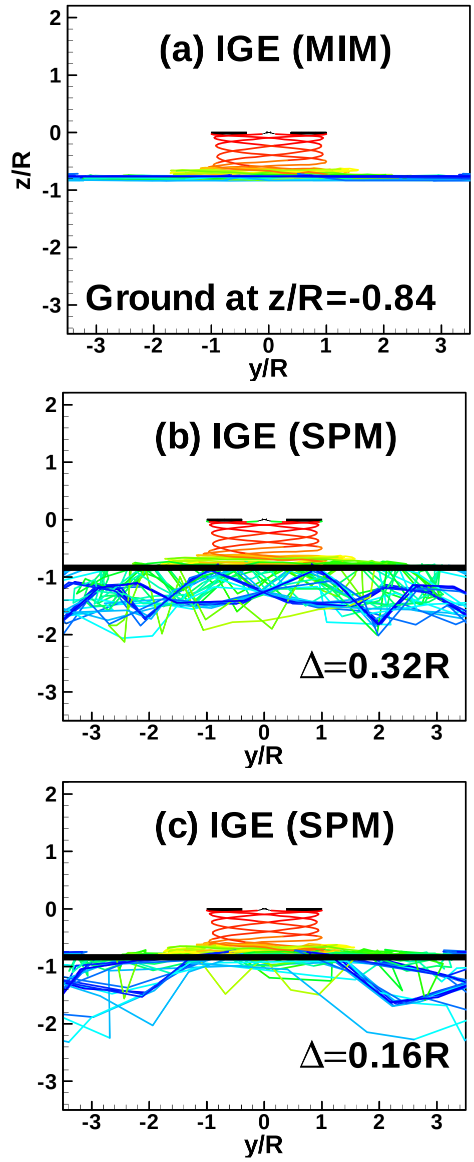

Fig. 10 Side view of the free wake for Lynx tail rotor hovering IGE (MIM) and IGE (SPM), showing vortex filaments penetration into the ground plane.

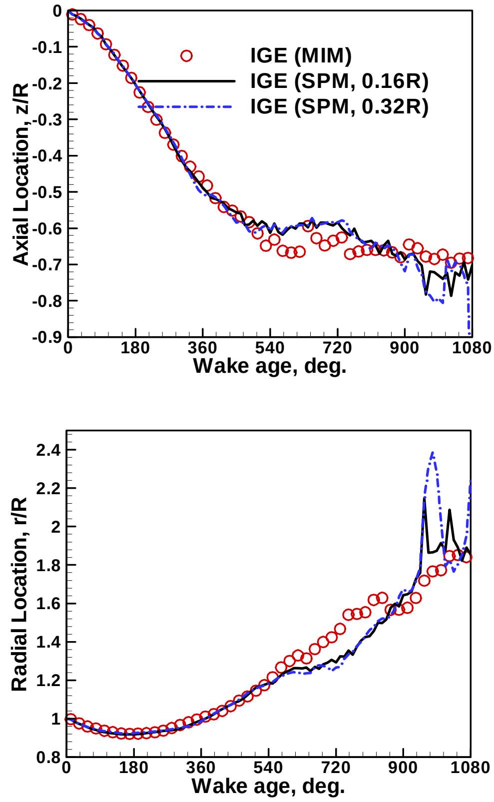

Fig. 11 Comparison of tip vortex axial and radial location IGE (MIM) and IGE (SPM)

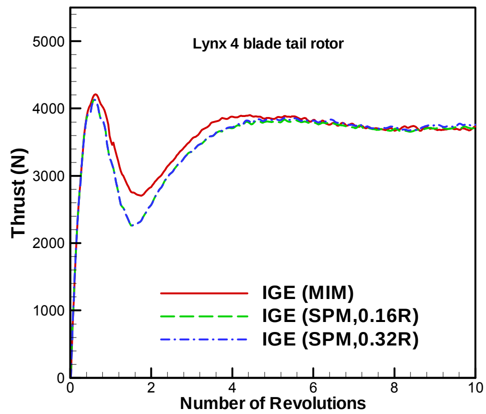

Fig. 12 Comparison of rotor thrust time history both IGE (MIM) and IGE (SPM)

The vortex filaments penetration into the ground plane is observed when the SPM model is used, as shown in Fig.10b, c. The ground plane marked as a straight black line is given in Fig.10b, c in order to give indication of wake leakage. Vortex filaments passing directly through a panelled fuselage were reported in the simulation of the wake fuselage interaction using a potential flow method [e.g. 8, 12]. Some special treatments to avoid this problem were also introduced in [12]. The comparison of **Fig.10b** and **10c** shows panel refinement can remedy the wake penetration, but with cost of computer memory capacity and CPU time. The dependence of the wake axial and radial locations on different panel density in the SPM and the comparison to MIM model is given in **Fig.11**. The wake penetration into the ground only affects the far-wake region, and therefore has only a small impact on the overall rotor performance. The large deviation occurs after the azimuthal angle of 540 deg. **Fig.12** compares rotor thrust time histories. It shows that after the start vortices move away from the blades and the normal wake structures are established, the thrust IGE converges to its final value. Only small deviations are observed among the results.

4.2 Main rotor (MR)/ Tail rotor (TR) IGE

2-blade MR and 2-blade TR IGE (MIM)

The MR is identical to the Caradonna and Tung rotor used in the previous section. The TR is a quarter scaled replica of the MR with same collective pitch as the MR and runs at twice the MR rpm. The TR axis lies in the plane of the MR disc. The MR and TR rotation planes were set normal to one another. Seen from the top, the MR rotates anti-clockwise and the advancing TR blade moves down (Advancing Side Down, ASD mode). The TR axis is located at 1.58 MR radii from the MR axis, which allows a gap of 0.33 MR radii between the blade tip trajectories of MR and TR.

An identical paneling scheme was used for the MR and the TR. The results were obtained for a MR azimuth step size of 11.25 degrees and both rotors were impulsively started at the same time.

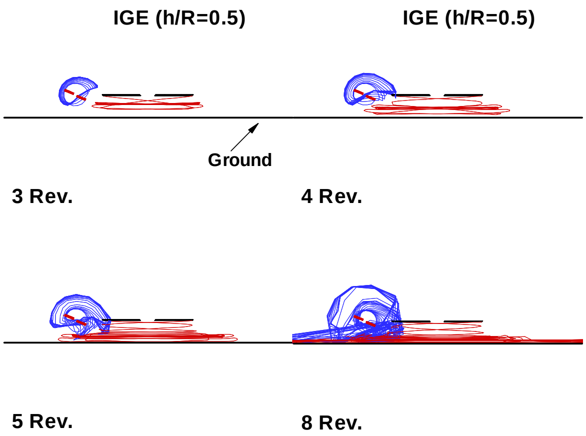

Fig. 13 Development of the tip vortex of two-bladed MR- and TR in hover IGE (h/R=0.5)

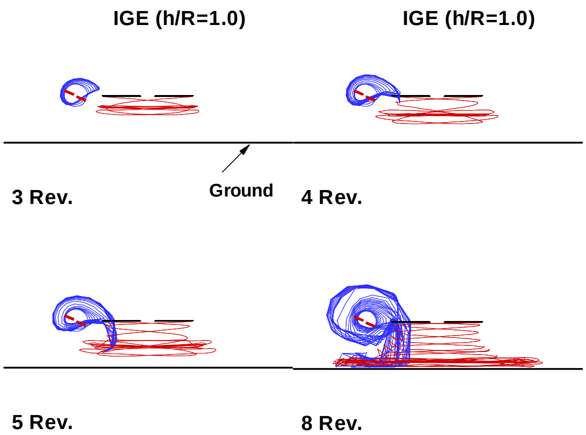

Fig. 14 Development of the tip vortex of two-bladed MR- and TR in hover IGE (h/R=1.0)

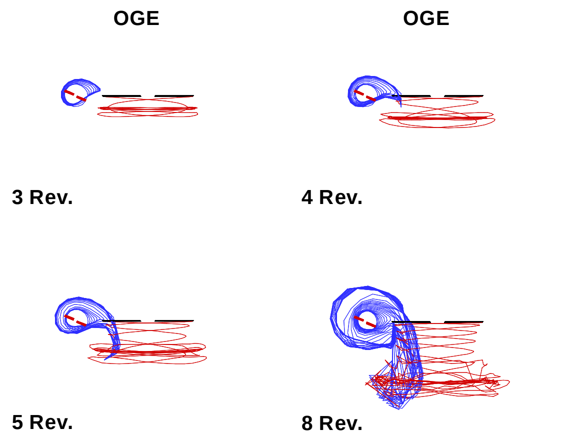

Fig. 15 Development of the tip vortex of two-bladed MR- and TR in hover OGE

Fig.13-15 illustrate the development of the MR and TR free wakes and their merging process for both IGE with different h/R and OGE in the sequence of different MR revolutions. The individual wakes remain separate until 4 revolutions IGE, but at the 4th revolution, the TR wake is already drawn into the MR wake OGE (**Fig.15**) because the MR induced velocity field is stronger in OGE. For small ground distance, a splitting of the TR tip vortex bundle is observed as shown in **Fig.13** at the subsequent revolution (5th Rev.). One part of the tail rotor tip vortex bundle has interacted with an outward part of the MR wake due to the induction from the edge of the main rotor tip vortex radially extended IGE. The other part of the TR tip vortex is drawn into the MR disc and interacts with the MR and its wake there. As the computation progresses, the strong induction of the MR wake distorts and finally absorbs the TR wake completely. Both MR and TR wake IGE is seen to spray out parallel to the ground plane.

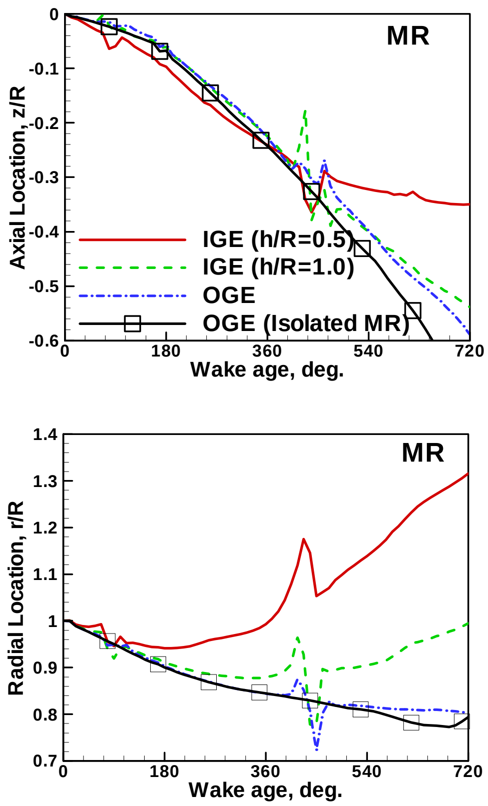

Fig. 16 Comparison of the MR wake axial and radial locations with respect to different h/R for MR/TR interaction IGE (MIM)

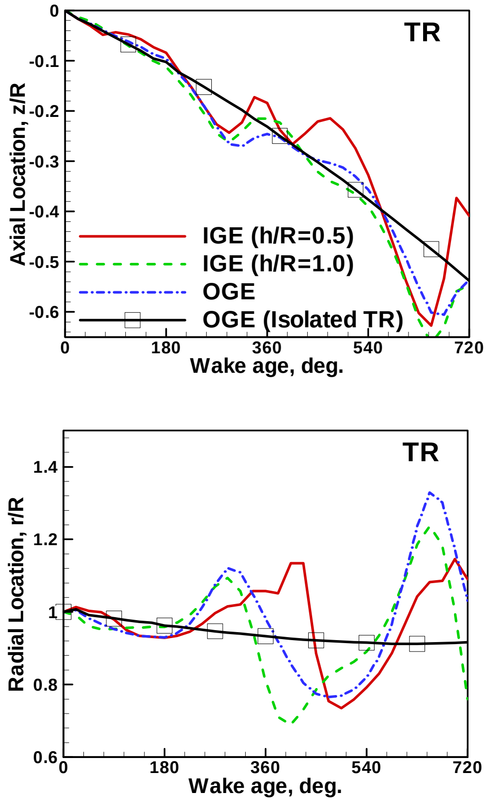

Fig. 17 Comparison of the TR wake axial and radial locations with respect to different h/R for MR/TR interaction IGE (MIM)

The comparison of the wake axial and radial locations between IGE and OGE is given in **Fig.16** for MR and **Fig.17** for the TR. For comparison, the results for the rotors in isolation are also drawn. It can be seen that the wake locations are deformed due to the MR and TR interaction and the existence of the ground again further enhance the deformation.

The variation of thrust over the azimuth can also be used to analyze the effect of ground on the MR/TR interaction process. **Fig.18** and **Fig.19** give comparison of the thrust time history for both MR and TR under the MR/TR interaction and ground effect.

It shows in general the averaged MR thrust increases with decreased rotor-ground distance. The one per rev peaks, which are caused by the main rotor cutting across or interacting with the tail rotor wake, are pronounced IGE.

Only a slight increase in the TR averaged thrust IGE is observed, but the variation of the peaks IGE are obvious. The peak group is duplicated twice per rev. corresponding to the selected r.p.m. ratio of the M- and TR. The relevant plot OGE highlights the ground effect.

The strong load fluctuations occurring for the MR and the TR during the hover flight condition may have adverse effects on the noise and vibrations.

It is worth mentioning here that this case of interacting rotor wakes cannot be simulated with a prescribed wake approach.

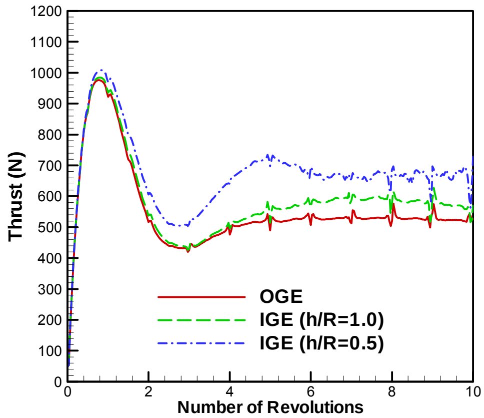

Fig. 18 Time history of MR thrust (Hover, both MR and TR in operation)

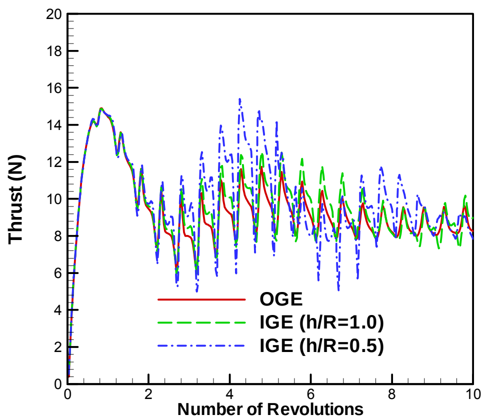

Fig. 19 Time history of MR thrust (Hover, both MR and TR in operation)

BO105 4-blade-MR and 2-blade TR in level flight IGE

BO105 MR and TR in level flight condition is simulated. BO105 has a 4-blade MR and a 2-blade TR. The MR blade with a NACA 23012 airfoil modified at trailing edge has -8° of linear twist, a square tip and a solidity of 0.077. The tip Mach number is $M_{Tip} = 0.64$. The advance ratio is 0.151. TR is equipped with two untwisted blades with S102E profile. The advancing side down (ASD) mode is selected as the rotational direction of the TR. The ratio of TR to MR rpm is set at 5.2.

An identical paneling scheme was used for the MR and the TR. The time resolution is 5° for MR and 26° for TR. The method of images is used to simulate the ground effect and the ground plane is located at z/R=-0.5.

To show the wake and ground interaction on the development of the MR/TR wakes in a level flight, a snap-shot of the free wakes results is demonstrated in **Fig.20**. The result when the rotors are operating OGE is also given for the comparison.

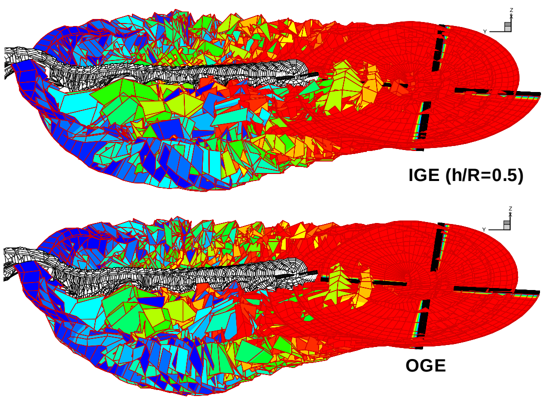

Fig. 20 Perspective view of MR and TR wakes IGE and OGE in level flight

Similar MR wake geometries are observed for operations OGE and IGE with slight wake extension laterally. The merging of the MR and TR wake is stronger IGE than OGE. The interaction of MR with its own wake is also stronger IGE than OGE, especially in advancing side area. The TR blade cuts across in MR wake. The MR blade passes close to the edge of the TR wake but does not intersect it.

The rear view of the wakes (seeing from downstream towards rotor hub) in **Fig.21** shows the similar behavior of the wake edge roll-up and the effect of the ground forces the far wake turning towards the rotational plane.

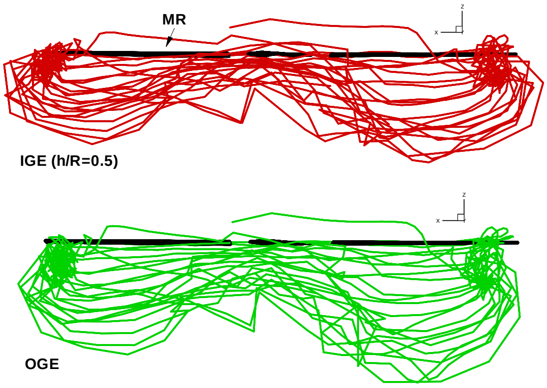

Fig. 21 Comparison of rear view of tip vortex of MR wake IGE and OGE (seeing from down-stream towards rotor hub)

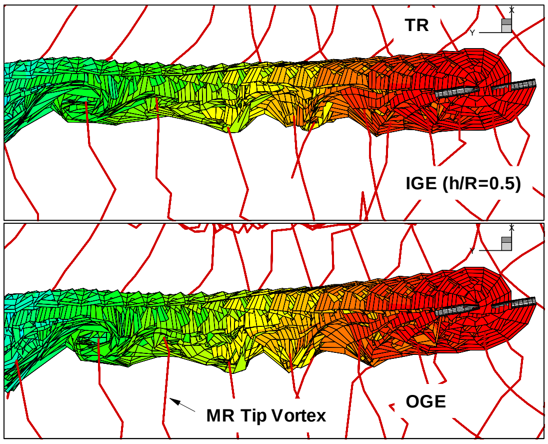

Fig. 22 Perspective view of TR wakes IGE and OGE including MR tip vortex trajectories (red solid line)

The perspective view of TR wakes IGE and OGE including MR tip vortex trajectories (red solid line in the plot) is given in **Fig.22**. The interaction of the MR/TR wake causes strong deformation on the lower side of the TR wake. The wake edge roll-up in up part of the TR wake is clearly demonstrated.

Fig.23 and **Fig.24** give the thrust time history for both MR and TR under the MR/TR interaction and ground effect. Slightly increasing mean MR thrust IGE is observed. The BVI peaks occurring in advancing and retreating side are pronounced IGE. The changing in the TR averaged thrust IGE can be neglected, although the enhancement of the TR interaction peaks IGE is obvious.

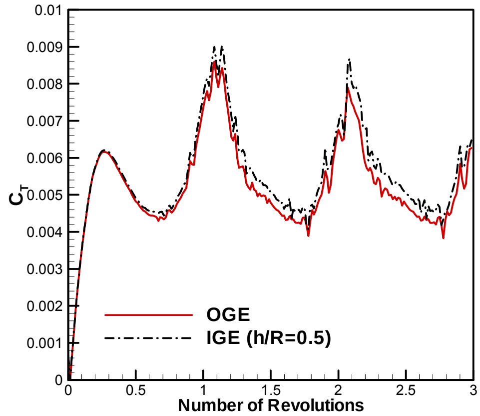

Fig. 23 Time history of MR thrust (Level flight, both MR and TR in operation)

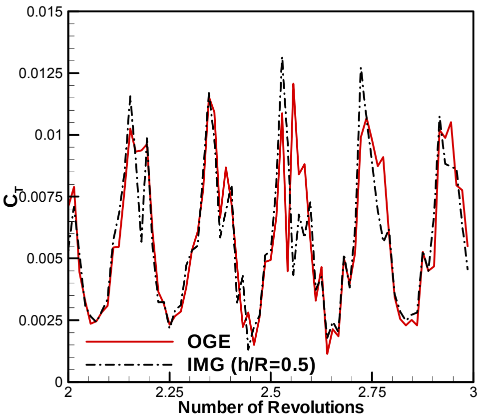

Fig. 24 Time history of TR thrust (Level flight, both MR and TR in operation)

Summary

This paper presents numerical results of the aerodynamics of a helicopter MR and TR operating under mutual interaction and ground effect. Configurations studied are a two-bladed MR and two-bladed TR in hover and a four-bladed MR and two-bladed TR in forward flight condition. The results with two different ground models are compared. The problem of using a surface singularity model is discussed.

REFERENCES

1. Quackenbush, T. R., Bliss, D.B. and Mahajan, A., "High Resolution Flow Field Prediction for Tail Rotor Aeroacoustics", 45th AHS Annual Forum, Boston, MA, May 1989.
2. Baron, M. and Boffadossi, M., "Unsteady Free Wake Analysis of Closely Interfering Helicopter Rotors", Paper No. 108, 19th European Rotorcraft Forum, Cernobbio, Italy, Sept. 14-16, 1993.
3. Bagai, A. and Leishman, G.J., "Free-Wake Analysis of Tandem, Tilt-Rotor and Coaxial Rotor Configurations", 51st AHS Annual Forum, Fort Worth, Texas, May 9-11, 1995.
4. Yin, J.P., Ahmed, S.R.: ´ Helicopter main-rotor/tail-rotor interaction', Journal of the American helicopter society, Vol. 45, No. 4, pp293-302, October 2000.
5. Balch,D.T., "Experimetal study of main rotor/tail rotor/airframe interaction in hover", 39th AHS Annual Forum, St. Louis, Missouri, May, 1983.
6. Griffiths, D.A. and Leishman, G.J., "A study of dual-rotor interference and ground effect using a free-vortex wake model", 58th AHS Annual Forum, Montreal, Canada, June 11-13, 2002.
7. Yin, J., Buchholz, H., and Splettstoesser, W., 'Numerical Simulation of Bo105 Main/Tail Rotor Interaction Noise And Preliminary Comparisons with Flight Test Results', 28th European Rotorcraft Forum,17 - 20 Sep. 2002, Bristol, England
8. Wachspress, D.A., Quackenbush, T. R., and Boschitsch, A.H., "Rotorcraft interactional aerodynamics calculations with fast vortex/fast panel methods", 56th AHS Annual Forum, Virginia Beach, Virginia, May 2000.
9. Light, J.S., "Tip vortex geometry of a hovering helicopter rotor in ground effect", 45th AHS Annual Forum, Boston, Massachusetts, May 22-24, 1989.
10. Caradonna, F.X. and Tung, C., "Experimental and Analytical Studies of a Model Helicopter Rotor in Hover", NASA TM 81232, 1981.
11. Cheeseman, I. and Bennett, W., "The effect of the ground on a helicopter rotor in forward flight", ARC R&M 3021, Sep 1955.
12. Clark, D. R., "A re-examination of the aerodynamics of hovering rotors including the presence of the fulage", International Technical Specialists' Meeting on Rotorcraft Basic Research, Atlanta, GA, 30332, March 25-27, 1991.